Strong transparent magnetic nanopaper prepared by immobilization of Fe$_3$O$_4$ nanoparticles in a nanofibrillated cellulose network†

Yuanyuan Li,‡[ab] Hongli Zhu,‡[b] Hongbo Gu,[c] Hongqi Dai,[a] Zhiqiang Fang,[b] Nicholas J. Weadock,[b] Zhanhu Guo*[c] and Liangbing Hu*[b]

Nanofibrillated cellulose (NFC) is highly regarded as a popular new material due to its impressive mechanical properties, great potential for functionalization, easy accessibility, and environmental sustainability as precursors. The immobilization of nanoparticles in an NFC network is an effective way to fabricate transparent functionalized nanopaper. In this work, a uniform, flexible, magnetic nanopaper is prepared by the immobilization of Fe$_3$O$_4$ nanoparticles in an NFC network in an aqueous medium. The resulting transparent magnetic nanopaper (TMNP) possesses excellent transparency and magnetic properties combined with outstanding mechanical performance and flexibility. The combination of these characteristics makes TMNP an excellent candidate for magneto-optical applications.

Introduction

Transparent magnetic materials play an important role in bioanalytical applications, magneto-optical switches, magneto-optical sensors, modulators, optical circulators, and optical isolators.[1–3] Preparation of transparent magnetic materials with excellent magnetic, optical, mechanical, and thermal properties has attracted great interest over the last twenty years.[4–7] A transparent magnetic thin polyvinyl alcohol (PVA) film is prepared by spin coating a solution of magnetite fine particles on glass substrates, and followed by drying at 80 °C and solidifying at 200 °C in a magnetic field.[4] Hyon Min Song obtained transparent magnetic composites by covalently bonding liquid crystals to the siloxane backbones and then linking them to dopamine-functionalized Fe$_3$O$_4$ nanocrystals.[5] Yibo Dou fabricated transparent magnetic films *via* layer-by-layer assembly of layered double hydroxide nanoplatelets, PVA and a styrylbiphenyl derivative.[6] Co-doping of TiO$_2$ thin films as well as selective oxidation of a metallic glass are also the reported methods to obtain transparent magnetic films.[7,8] The main design approach is to embed magnetic particles into a transparent matrix, such as polymers, silica gels, glass, and ion exchange resins.[9–13]

Embedding magnetic particles into a transparent matrix is a relatively easy procedure and the resulting composites provide necessary stability and processability for applications. However, the challenge for this method is that magnetic particles are unable to be uniformly dispersed in the organic matrix due to agglomeration.[13] Only a low concentration of magnetic particles can be dispersed in the matrix, resulting in high transparency but poor magnetic properties. Recently, the stability of high quality magnetic particles has been increased through the use of monomeric stabilizers, or by coating iron oxide nanoparticles with inorganic particles (silica or gold) and organic polymers (like PVA, alginate and chitosan).[14,15] *In situ* synthesis of magnetic particles is another way to reduce agglomeration during composite processing because the aggregation of nanoparticles is prevented *via* the organic matrix and modification.[9,16] The magnetic and optical properties of magnetic nanocomposites mainly depend on the magnetic particle size and magnetic particle loading. Nanosized particles are favored in the transparent nanocomposite preparation because the particle size is smaller than the wavelength of visible light. Small diameter magnetic particles with a narrow size distribution are important to guarantee transparency and favorable magnetic properties. Additionally, a higher concentration of magnetic particles in the matrix maintains good magnetic properties, but decreases transparency.

The mechanical properties of magnetic nanocomposites also need to be taken into account for applications. The mechanical properties are mainly determined by the matrix material. Nanocellulose prepared from plant, bacteria, or selected marine creatures is being praised for its high aspect ratio, high specific

[a]College of Light Industry Science and Engineering, Nanjing Forestry University, Nanjing, Jiangsu 210037, P. R. China

[b]Department of Materials Science and Engineering, University of Maryland College Park, MD 20740, USA. E-mail: binghu@umd.edu

[c]Integrated Composites Lab (ICL), Dan F. Smith Department of Chemical Engineering, Lamar University, Beaumont, TX 77710, USA. E-mail: zhanhu.guo@lamar.edu

† Electronic supplementary information (ESI) available: A video detailing the switching process of magnetic paper for illuminating an LED. See DOI: 10.1039/c3ta12591b

‡ Equal contribution.

surface area, impressive mechanical properties, and low weight.[17–24] 2,2,6,6-Tetramethylpiperidine-1-oxyl (TEMPO) oxidized nanocellulose is stable in water without aggregation due to the introduction of charged groups (–COO$^-$) on the fiber surface.[25] The charged groups and hydroxyl groups decorating the nanocellulose surface are sites for chemical functionalization and adsorption of polymers and particles through electrostatic forces and hydrogen bonding.[26–28] R. T. Olsson prepared magnetic aerogels using freeze-dried bacterial cellulose nanofibril aerogels as templates to adsorb metal ions for $CoFe_2O_4$ in situ synthesis.[29] Another emerging application of nanocellulose is making transparent paper for electronic device substrates.[30] The biocompatibility of nanocellulose makes it suitable for life science applications including use with human fibroblasts.[31] Nanocellulose forms a three-dimensional (3D) network in the paper, which is good for the immobilization of particles. Based on these concepts, we fabricated highly transparent free-standing magnetic nanopaper with excellent mechanical and magnetic properties. Nanofibrillated cellulose (NFC) was first used as a stabilizer for Fe_3O_4 NPs to make uniformly dispersed, stable Fe_3O_4 NPs in aqueous medium. The transparency, tensile strength and magnetic properties of the transparent magnetic nanopaper (TMNP) are some of the highest reported values among recently prepared TMNPs. The excellent properties and green and biocompatible nature of our TMNP have great potential in applications including magneto-optical applications, electromagnetic shielding, and in vitro magnetic separation in the life sciences.[11,32,33]

Experimental

Magnetic nanoparticles and NFC preparation

Fe_3O_4 nanoparticles (NPs) were obtained from Nanjing Emperor Nano Material Co., Ltd., China. The particles are spheres with an average particle size of 20 nm, and a specific surface area of greater than 60 m^2 g^{-1}.

NFC was prepared according to an existing method.[34] Briefly, TEMPO (78 mg), sodium bromide (NaBr, 514 mg) and 5 g Kraft bleached softwood pulp were mixed together. TEMPO oxidation of cellulose was triggered by adding sodium hypochlorite (NaClO) at room temperature under gentle agitation. During the oxidation process, the pH was maintained at 10.5. After TEMPO treatment, the fibers were thoroughly washed with distilled water and disintegrated by one pass through a Microfluidizer M-110EH (Microfluidics Ind., USA) to obtain a NFC suspension.
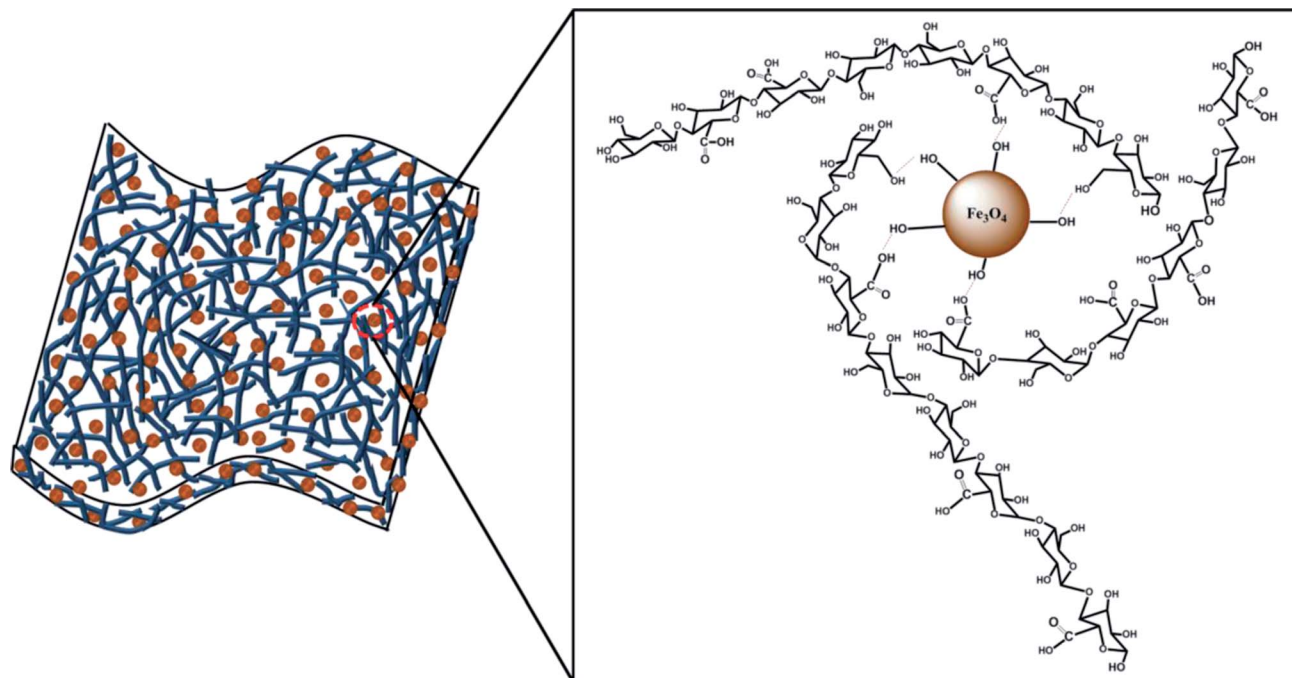
Transparent magnetic nanopaper preparation

First, NFC and Fe_3O_4 NPs were uniformly dispersed and mixed together with weight ratios of 95 : 5, 90 : 10 and 80 : 20 for transparent magnetic paper samples containing different Fe_3O_4 loadings. The resulting dispersion was poured into a Buchner funnel for filtration. Finally, a gel cake formed on top of the filter membrane, and the cake was dried under pressure. After drying, magnetic nanopaper samples with a diameter of 90 mm were obtained. The paper thickness and diameter were easily tailored by controlling the mixture volume and filter size in the paper forming process. The transmittance of TMNP was analyzed with

a Lambda 35 UV-Vis Spectrometer (PerkInElmer, USA). The tensile strength of the TMNP was characterized with a Tinius Olsen H25KT universal material strength testing machine. Each specimen was cut into a strip of 5 mm × 50 mm.

Results and discussion

The optical transmittance, magnetic properties, and mechanical properties of optical composites are particle size dependent; a smaller particle size will improve light transmittance and magnetic and mechanical performance. Smaller particles, however, possess a higher specific surface area and as a result are more prone to agglomeration.[35] Thus, a uniform dispersion of magnetic particles with a smaller size in an NFC suspension is critical for tuning the desired properties of functionalized nanopaper. Scheme 1 illustrates the TMNP structure. In this work, Fe_3O_4 NPs are immobilized in an NFC fiber network through interactions between carboxyl groups/hydroxyl groups of NFC and surface hydroxyl groups of Fe_3O_4 NPs.[36,37] The Fe_3O_4 NPs used are spherical with an average particle size of 20 nm. The prepared NFC is about 10 nm in diameter and hundreds of nanometers long, as measured using a transmission electron microscope (TEM) (Fig. 1 a). After TEMPO oxidation, large amounts of charged carboxyl groups (–COO$^-$) are introduced onto the surface of the NFC fibers. The surface carboxyl groups generate repulsive forces between NFC fibers, making them stable in water without aggregation. The TMNP is made by first adsorbing the Fe_3O_4 NPs onto the NFC fibers in solution and then filtering out the solvent. The Fe_3O_4 NPs are easily adsorbed onto NFC, and the repulsive forces generated by surface carboxyl groups between NFC fibers provide stability in water. During filtration, NFC deposits on the filter paper and forms a 3D gel network, with the magnetic particles wrapped by NFC. A final drying step fixes the magnetic particles within the fiber network. The surface carboxyl groups and hydroxyl groups in the formed fiber network make NFC an excellent matrix for immobilization of not only Fe_3O_4 NPs but also other nanoparticles as well. This method will allow for the functionalization of nanopaper with a wide range of nanomaterials. Here, the NFC also acts as a dispersant and a stabilizer for Fe_3O_4 NPs in water. We prepared 0.2 wt% Fe_3O_4 NP water solutions with 10 wt% NFC (relative to the Fe_3O_4 NP weight) to investigate the stability of the solution. The Fe_3O_4 NP/NFC solution was stable after 20 days, whereas Fe_3O_4 NP solutions without NFC settled out and the solution became clear as observed in Fig. 1(b). The obtained TMNP is 26 μm thick with Fe_3O_4 NPs uniformly dispersed. Fig. 1(c) shows the cross-section of TMNP and Fig. 1(d) is the element map of Fe in the TMNP cross-section. Fe uniformly dispersed throughout the cross-section indicates the uniform dispersion of Fe_3O_4 NPs in the whole paper.

The fabricated TMNP is transparent in visible light with excellent flexibility. In Fig. 2(a) the words "cellulose paper" are clearly visible under the bent paper. This is attributed to the excellent transmittance of nanopaper. Reducing the diameter of paper fibers will decrease optical scattering, improving the transparency of paper.[34] Pure nanopaper composed of fibers

Scheme 1 Schematic of transparent magnetic nanopaper, Fe_3O_4 NPs are immobilized in the 3D NFC network (left) through interactions between carboxyl groups/ hydroxyl groups of NFC and surface hydroxyl groups of Fe_3O_4 NPs (right).
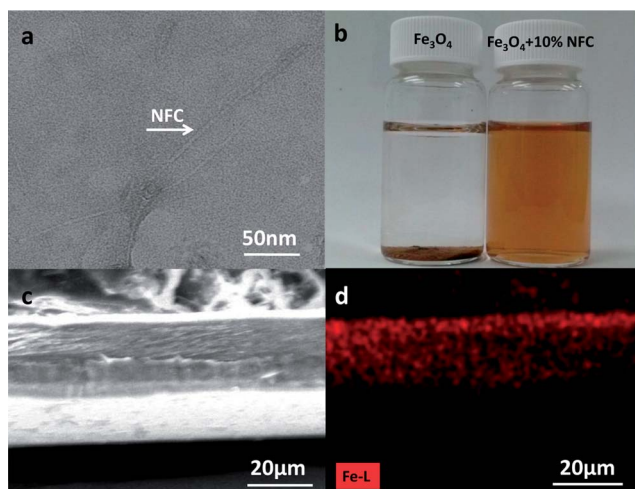

Fig. 1 (a) TEM image of NFC, (b) Fe_3O_4 NP solution without (left) and with (right) NFC, after 20 days of preparation, (c) SEM images of TMNP cross-section, and (d) Fe element mapping of TMNP cross-section.

Fig. 2 (a) A digital image of magnetic paper with 10 wt% Fe_3O_4 NPs shows the transparency and flexibility, (b) nanopapers with 0 wt%, 5 wt%, and 10 wt% Fe_3O_4 NP loading from left to right and (c) transmittance curves of magnetic papers.

with a diameter on the order of 10 nm possesses a high transmittance of 93% at a wavelength of larger than 550 nm.[38] Nanopaper also possesses a 3D fiber network structure with high flexibility.[39] The Fe_3O_4 NPs are uniformly fixed in the network through chemical bonding and mechanical wrapping. The transparency of the magnetic nanopaper can be tailored by Fe_3O_4 NP loading. Nanopaper with a lower Fe_3O_4 NP loading exhibits higher transparency. As the weight ratio of Fe_3O_4 NPs is increased from 0 to 10%, the letters beneath the paper are more obscured, as shown in Fig. 2(b). At the
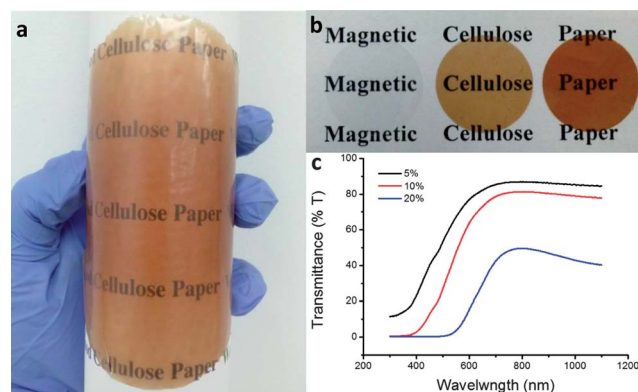
same time, the color changes from light yellow to dark brown, due to the dark color of Fe_3O_4 NPs. Fig. 2(c) shows the transmittance curves of three TMNP samples. As the Fe_3O_4 NP loading increases, the transmittance decreases in the 350–1100 nm wavelength region. This is mainly due to the optical absorption of Fe_3O_4 NPs.[40] The highest transmittance is 86%, which is good enough to be applied in transparent magnetic devices.

An entire TMNP sample with a Fe_3O_4 NP loading of 10% is easily lifted with a household magnet, as shown in Fig. 3(a). In addition, the TMNP is writable; conductive ink can be used to write on it through a ballpoint pen as shown in Fig. 3(b). The TMNP with a written circuit is an excellent magnetic switch as
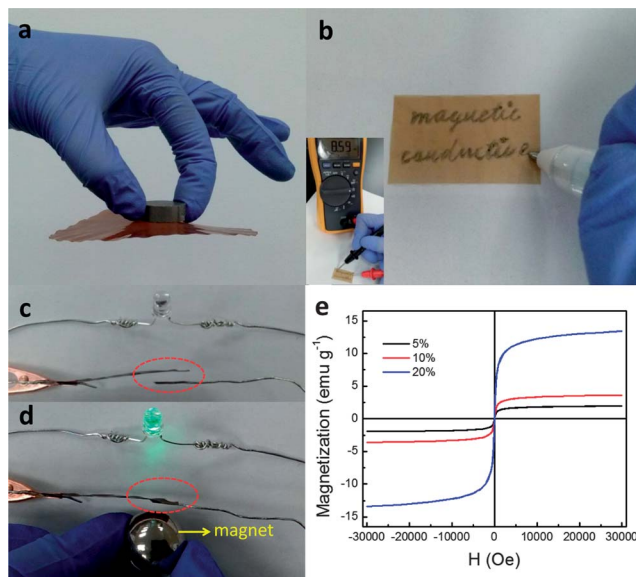
15280 | J. Mater. Chem. A, 2013, **1**, 15278–15283

This journal is © The Royal Society of Chemistry 2013

Fig. 3 (a) shows that a 90 mm diameter magnetic paper with 10 wt% Fe_3O_4 NPs loading can be easily lifted with a household magnet, (b) shows the magnetic nanopaper with CNT ink written on it, with the inset demonstrating the conductivity of the ink on TMNP, the paper contains 5 wt% Fe_3O_4 NPs, (c) and (d) show the magnetic switch, there is a gap between conductive magnetic paper and nonmagnetic Sn wire (c), when a magnet was placed close to the conductive magnetic paper, the paper moved to contact with Sn wire and lighted the LED, the TMNP possesses 20 wt% Fe_3O_4 NPs, (e) plots the magnetization curves of TMNPs measured at room temperature.

illustrated in Fig. 3(c) and (d). The TMNP switch is actuated when a magnet is closer, illuminating an LED connected to the switch with a nonmagnetic Sn wire. A video of the switch actuation to illuminate the LED is provided in the ESI.† Magnetization curves of all samples were investigated using a 9-Tesla Physical Properties Measurement System (Quantum Design) at room temperature. The magnetization curves plotted are shown in Fig. 3(d). Magnetic NPs with a diameter on the order of 10 nm (depending on the materials) may exhibit a superparamagnetic state, or a state when the coercive force (H_c) is zero. The H_c of all the samples is zero Oe, indicating a superparamagnetic behavior. The magnetic properties in a superparamagnetic system can be described according to the Langevin equation (1):[41]

$$\frac{M}{M_s} = \coth x - \frac{1}{x} \quad (1)$$

where M is the magnetization (emu g^{-1}) in a magnetic field H (Oe), M_s is the saturation magnetization, and $x = aH$. The parameter a is a function of the electron spin magnetic moment μ (J T^{-1} or μ_B) of the individual molecule as described in eqn (2):

$$a = \frac{\mu}{k_B T} \quad (2)$$

Here, k_B is Boltzmann's constant, and T is the absolute temperature. The direction of a magnetic moment follows the direction of the applied magnetic field, and the magnetization increases with the increasing magnetic field until it reaches the saturation magnetization.[42] According to

Fig. 3(e), the magnetization of all the samples did not saturate for the applied magnetic field. The M_s is obtained from the intercept of $M \sim H^{-1}$ at a high magnetic field Fig. 3(e).[43] The M_s of the as-received Fe_3O_4 NPs is 62.99 emu g^{-1}, which is smaller than that of bulk Fe_3O_4 (92 emu g^{-1}).[44] The M_s of the TMNP with Fe_3O_4 NP loading of 5, 10, and 20 wt% are 2.04, 3.80, and 14.17 emu g^{-1}, respectively. A higher loading of Fe_3O_4 NPs in nanopaper better maintains the saturation magnetization.

The best fit to eqn (1) is obtained by a nonlinear fitting of M and H using the Polymath software. The a for the as-received Fe_3O_4 NPs and magnetic paper with a Fe_3O_4 nanoparticle loading of 5, 10, and 20 wt% is 3.24×10^{-3}, 3.63×10^{-3}, 3.46×10^{-3}, and 3.32×10^{-3} T^{-1}, respectively. According to eqn (2), the magnetic moment μ can be calculated from a. The μ of the as-received Fe_3O_4 NPs and TMNP with Fe_3O_4 NP loadings of 5, 10, and 20 wt%, is 1.41, 1.56, 1.49, and 1.43 μ_B, respectively. The calculated μ does not change much between the four samples, indicating that NFC has little effect on the magnetic moment of the Fe_3O_4 NPs.

Another noticeable property of the transparent magnetic paper is the outstanding mechanical strength. The mechanical strength of cellulose paper is mainly affected by fiber orientation, fiber strength and the bonding strength between fibers. Nanocellulose paper possesses an extraordinarily high modulus of 10 GPa, due to the abundant hydroxyl groups on the surface.[45] The tensile strength of pure nanopaper is 213.5 MPa. When Fe_3O_4 NPs are added into nanopaper, they reduce the hydrogen bonding between fibers and decrease both the tensile strength and elastic modulus. Increasing the Fe_3O_4 NP loading further reduces the strength and elastic modulus. The relationship between the Fe_3O_4 NP and their mechanical properties is presented in Fig. 4(a). However, the TMNP still possesses a high strength and elastic modulus. TMNP with Fe_3O_4 NP loadings of 5, 10, and 20 wt% possesses tensile strengths of 171.3, 137.8, and 120.4 MPa, respectively. This is the highest strength reported for transparent magnetic films and magnetic paper.[1,46] The elastic modulus of TMNP with a Fe_3O_4 NP loading of 0, 5, 10, and 20 wt% is 10.7, 8.3, 7.7 and 7.1 GPa, respectively. The high strength broadens the application of TMNP. Fig. 4(b) shows the cross-section of TMNP after breaking. The TMNP exhibits a layered structure similar to pure nanopaper. After failure, the NFC fibers at the failure site are aligned parallel to the pulling direction.
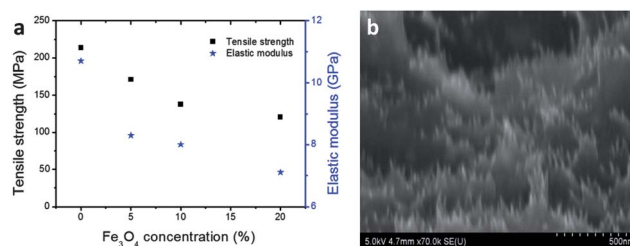

Fig. 4 (a) Average tensile strength and elastic modulus of TMNP with various Fe_3O_4 NP loadings, and (b) the SEM image of TMNP cross-section after breaking.

This journal is © The Royal Society of Chemistry 2013

J. Mater. Chem. A, 2013, **1**, 15278–15283 | **15281**

Conclusion

In summary, highly transparent magnetic nanopaper was fabricated by immobilization of magnetic particles in a nanocellulose fiber network. The optical, magnetic, and mechanical properties depend on the concentration of magnetic particles in the paper. The obtained magnetic paper is transparent in visible light with a high transmittance of 86% and possesses an excellent tensile strength of 171.3 MPa. Combining these outstanding properties with low cost, green, cellulose fibers and a relatively simple manufacturing procedure makes this material an excellent candidate for magneto-optical applications.[47]

Acknowledgements

Notes and references

1 S. Thomas, D. Sakthikumar, P. A. Joy, Y. Yoshida and M. R. Anantharaman, *Nanotechnology*, 2006, **17**, 5565–5572.
2 P. C. Gach, C. E. Sims and N. L. Allbritton, *Biomaterials*, 2010, **31**, 8810–8817.
3 P. Patoka, T. Skeren, M. Hilgendorff, L. J. Zhi, T. Paudel, K. Kempa and M. Giersig, *Small*, 2011, **7**, 3096–3100.
4 K. Yamaguchi, K. Matsumoto and T. Fujii, *J. Appl. Phys.*, 1990, **67**, 4493–4495.
5 H. M. Song, J. C. Kim, J. H. Hong, Y. B. Lee, J. Choi, J. I. Lee, W. S. Kim, J. H. Kim and N. H. Hur, *Adv. Funct. Mater.*, 2007, **17**, 2070–2076.
6 Y. B. Dou, X. X. Liu, M. F. Shao, J. B. Han and M. Wei, *J. Mater. Chem. A*, 2013, **1**, 4786–4792.
7 N. C. D. V. Louzguine-Luzgin, T. Hitosugi, S. V. Ketov, A. Shluger, V. Y. Zadorozhnyy, A. Caron, S. Gonzales, C. L. Qin and A. Inoue, *Thin Solid Films*, 2013, 471–475.
8 A. Lopez-Santiago, P. Gangopadhyay, J. Thomas, R. A. Norwood, A. Persoons and N. Peyghambarian, *Appl. Phys. Lett.*, 2009, **95**, 143302.
9 J. G. Moore, E. J. Lochner, C. Ramsey, N. S. Dalal and A. E. Stiegman, *Angew. Chem., Int. Ed.*, 2003, **42**, 2741–2743.
10 M. Z. Zayat, F. del Monte, M. D. Morales, G. Rosa, H. Guerrero, C. J. Serna and D. Levy, *Adv. Mater.*, 2003, **15**, 1809–1812.
11 R. F. Ziolo, E. P. Giannelis, B. A. Weinstein, M. P. Ohoro, B. N. Ganguly, V. Mehrotra, M. W. Russell and D. R. Huffman, *Science*, 1992, **257**, 219–223.
12 Y. Matsumoto, M. Murakami, T. Shono, T. Hasegawa, T. Fukumura, M. Kawasaki, P. Ahmet, T. Chikyow, S. Koshihara and H. Koinuma, *Science*, 2001, **291**, 854–856.
13 K. Hayashi, R. Fujilkawa, W. Sakamoto, M. Inoue and T. Yogo, *J. Phys. Chem. C*, 2008, **112**, 14255–14261.
14 S. Laurent, D. Forge, M. Port, A. Roch, C. Robic, L. V. Elst and R. N. Muller, *Chem. Rev.*, 2008, **108**, 2064–2110.
15 C. Yang, J. J. Wu and Y. L. Hou, *Chem. Commun.*, 2011, **47**, 5130–5141.
16 E. M. Moreno, M. Zayat, M. P. Morales, C. J. Serna, A. Roig and D. Levy, *Langmuir*, 2002, **18**, 4972–4978.
17 M. Martinez-Sanz, A. Lopez-Rubio and J. M. Lagaron, *Carbohydr. Polym.*, 2011, **85**, 228–236.
18 S. Elazzouzi-Hafraoui, Y. Nishiyama, J. L. Putaux, L. Heux, F. Dubreuil and C. Rochas, *Biomacromolecules*, 2008, **9**, 57–65.
19 A. Isogai, T. Saito and H. Fukuzumi, *Nanoscale*, 2011, **3**, 71–85.
20 R. J. Moon, A. Martini, J. Nairn, J. Simonsen and J. Youngblood, *Chem. Soc. Rev.*, 2011, **40**, 3941–3994.
21 J. Huang, H. L. Zhu, Y. C. Chen, C. Preston, K. Rohrbach, J. Cumings and L. B. Hu, *ACS Nano*, 2013, **7**, 2106–2113.
22 Q. Q. Wang, J. Y. Zhu, R. S. Reiner, S. P. Verrill, U. Baxa and S. E. McNeil, *Cellulose*, 2012, **19**, 2033–2047.
23 M. Stromme, A. Mihranyan and R. Ek, *Mater. Lett.*, 2002, **57**, 569–572.
24 M. Stromme, A. Mihranyan, R. Ek and G. A. Niklasson, *J. Phys. Chem. B*, 2003, **107**, 14378–14382.
25 T. Saito, S. Kimura, Y. Nishiyama and A. Isogai, *Biomacromolecules*, 2007, **8**, 2485–2491.
26 S. J. Eichhorn, A. Dufresne, M. Aranguren, N. E. Marcovich, J. R. Capadona, S. J. Rowan, C. Weder, W. Thielemans, M. Roman, S. Renneckar, W. Gindl, S. Veigel, J. Keckes, H. Yano, K. Abe, M. Nogi, A. N. Nakagaito, A. Mangalam, J. Simonsen, A. S. Benight, A. Bismarck, L. A. Berglund and T. Peijs, *J. Mater. Sci.*, 2010, **45**, 1–33.
27 Z. Liu, H. S. Wang, B. Li, C. Liu, Y. J. Jiang, G. Yu and X. D. Mu, *J. Mater. Chem.*, 2012, **22**, 15085–15091.
28 A. Kumar, H. Gullapalli, K. Balakrishnan, A. Botello-Mendez, R. Vajtai, M. Terrones and P. M. Ajayan, *Small*, 2011, **7**, 2173–2178.
29 R. T. Olsson, M. Samir, G. Salazar-Alvarez, L. Belova, V. Strom, L. A. Berglund, O. Ikkala, J. Nogues and U. W. Gedde, *Nat. Nanotechnol.*, 2010, **5**, 584–588.
30 L. Nyholm, G. Nystrom, A. Mihranyan and M. Stromme, *Adv. Mater.*, 2011, **23**, 3751–3769.
31 N. Ferraz, M. Stromme, B. Fellstrom, S. Pradhan, L. Nyholm and A. Mihranyan, *J. Biomed. Mater. Res., Part A*, 2012, **100A**, 2128–2138.
32 V. C. Parveen Saini, N. Vijayan and R. K. Kotnala, *J. Phys. Chem. C*, 2012, 13403–13412.
33 T. C. Lin, F. H. Lin and J. C. Lin, *Acta Biomater.*, 2012, **8**, 2704–2711.
34 H. L. Zhu, S. Parvinian, C. Preston, O. Vaaland, Z. C. Ruan and L. B. Hu, *Nanoscale*, 2013, **5**, 3787–3792.

15282 | *J. Mater. Chem. A*, 2013, **1**, 15278–15283

This journal is © The Royal Society of Chemistry 2013

35 Y. A. Bamakov, B. L. Scott, V. Golub, L. Kelly, V. Reddy and K. L. Stokes, *J. Phys. Chem. Solids*, 2004, **65**, 1005–1010.

36 X. L. Chen, L. Li, X. M. Sun, Y. P. Liu, B. Luo, C. C. Wang, Y. P. Bao, H. Xu and H. S. Peng, *Angew. Chem., Int. Ed.*, 2011, **50**, 5486–5489.

37 S. S. Banerjee and D. H. Chen, *Nanotechnology*, 2009, **20**, 185103.

38 Z. X. Hongli Zhu, D. Liu, Y. Li, N. J. Weadock, Z. Fang, J. Huang and L. Hu, *Energy Environ. Sci.*, 2013.

39 W. Zhang, X. D. Zhang, C. H. Lu, Y. J. Wang and Y. L. Deng, *J. Phys. Chem. C*, 2012, **116**, 9227–9234.

40 A. Schlegel, S. F. Alvarado and P. Wachter, *J. Phys. C: Solid State Phys.*, 1979, **12**, 1157–1164.

41 H. B. Gu, Y. D. Huang, X. Zhang, Q. Wang, J. H. Zhu, L. Shao, N. Haldolaarachchige, D. P. Young, S. Y. Wei and Z. H. Guo, *Polymer*, 2012, **53**, 801–809.

42 H. W. Jiang Guo, H. Gu, Q. Zhang, N. Haldolaarachchige, Y. Li, D. P. Young, S. Wei and Z. Guo, *J. Phys. Chem. C*, 2013, **117**, 10191–10202.

43 D. Zhang, A. B. Karki, D. Rutman, D. R. Young, A. Wang, D. Cocke, T. H. Ho and Z. H. Guo, *Polymer*, 2009, **50**, 4189–4198.

44 N. S. Singh, D. R. Rodrigues and S. K. Dhawan, *Sci. Technol. Adv. Mater.*, 2003, **4**, 105–113.

45 A. Kulachenko, T. Denoyelle, S. Galland and S. B. Lindstrom, *Cellulose*, 2012, **19**, 793–807.

46 Y. Zheng, J. X. Yang, W. L. Zheng, X. Wang, C. Xiang, L. Tang, W. Zhang, S. Y. Chen and H. P. Wang, *Mater. Sci. Eng., C*, 2013, **33**, 2407–2412.

47 A. V. Kimel, A. Kirilyuk, P. A. Usachev, R. V. Pisarev, A. M. Balbashov and T. Rasing, *Nature*, 2005, **435**, 655–657.

This journal is © The Royal Society of Chemistry 2013

J. Mater. Chem. A, 2013, **1**, 15278–15283 | **15283**